Article:

Zhang, C. orcid.org/0000-0002-6719-7026, Guo, H., Jung, K. et al. (2 more authors) (2019) Screw reinforcement on dowel-type moment-resisting connections with cracks. Construction and Building Materials, 215. pp. 59-72. ISSN 0950-0618

https://doi.org/10.1016/j.conbuildmat.2019.04.160

Title: Screw reinforcement on dowel-type moment-resisting connections with cracks

Author names and affiliations:
Cong Zhang[a], Haibo Guo[b], Kiho Jung[c], Richard Harris[d], Wen-Shao Chang[e]

[a]Department of Architecture and Civil Engineering, University of Bath, Bath, UK
c.zhang@bath.ac.uk
[b]School of Architecture, Harbin Institute of Technology, Harbin, China
guohb@hit.edu.cn
[c]Faculty of Education, University of Shizouka, Shizouka, Japan
ekjung@ipc.shizuoka.ac.jp
[d]Time For Timber Ltd, Bath, UK
r.harris@timefortimber.co.uk
[e]Sheffield School of Architecture, University of Sheffield, Sheffield, UK
w.chang@sheffield.ac.uk

Corresponding author:

Wen-Shao Chang
Sheffield School of Architecture, University of Sheffield, Sheffield, UK
w.chang@sheffield.ac.uk

Abstract

This study uses partially threaded self-tapping screws to enhance the mechanical properties of damaged and undamaged dowel-type timber connections. The damaged connections have a 1.5mm wide artificial crack across the middle row of the fasteners. Test results showed that screw reinforcement can restore the rotation capacity of damaged connections. The rotational capacity of reinforced connections without cracks is 45.6% higher than unreinforced connections while the improvement on moment-resisting capacity is slight. Digital image correlation (DIC) was used to detect the movement of the connections and validated that the fasteners rotate around the centre of rotation in reinforced connections. Screw reinforcement also demonstrated the ability to control crack propagation, with the reinforced groups showed a reduction of crack length by at least 37% when compared to the unreinforced groups. A calculation method is proposed to calculate the characteristic moment-resisting capacity of damaged and undamaged screw reinforced connections. The calculated values are proven to be conservative when compared with the characteristic value based on the experimental results.

Highlights

- Self-tapping screws restored the rotational capacity of connections with cracks
- Partially threaded screws showed a trend to effectively control crack propagation
- A theoretical prediction method is demonstrated

Keywords

Self-tapping screws, reinforcement, timber dowel-type connections, moment-resisting, theoretical prediction

1. Introduction

Dowel-type connections are widely used in timber construction. As timber is weak in transferring load perpendicular to the grain, international standards have set ground rules to prevent splitting by limiting the minimum fastener spacing, end and edge distance in design. However, cracks can occur to existing timber connections due to moisture fluctuations. As the relative humidity varies in the environment, the wood tends to change its moisture content to achieve a balance. The material will change in size as it swells (increase in moisture content) or shrinks (decrease in moisture content). As the dimension of the wood changes, the fasteners in the connections tend to restrain this movement and stress will be concentrated in the wood around the fasteners. Excessive stresses can lead to cracking of the timber member and reduce the moment-resisting capacity and ductility of the connections. The moment-resisting capacity and ductility of a connection is usually critical, especially for high-rise timber buildings and structures in seismically active areas.

Studies [1-3] have used steel plates and FRPs (fibre-reinforced polymers) as reinforcement to repair damaged timber members. However, both reinforcement methods require a large amount of work and involve complex installation procedures. In addition, when such reinforcement is to be placed on the timber member, accessibility to a large surface area of the structural components is usually required and this can limit their application when repairing certain historical buildings.

Recent studies have indicated the potential use of self-tapping screws as reinforcement to dowel-type connections [4-6]. Their work shows that self-tapping screws can effectively reduce the splitting tendency of the connections. Other studies investigated the effectiveness of using self-tapping screws as reinforcement in bolted timber connections under dynamic load [7-10]. Lam, Gehloff and Closen [9] reported that screw reinforcement increased the moment-resisting capacity by 170% under reverse cyclic loading. In addition, self-tapping screws are easy to install and are less intrusive. A practical use of self-tapping screws to repair cracked dowel-type connections is shown in Figure 1.

Previous studies have investigated the influence of thread configuration of self-tapping screws as reinforcement to dowel-type connections [11, 12]. The results indicated that screws with 33% thread on the point end achieved similar performance as reinforcement to that of screws with complete thread. The studies suggested using partially threaded screws, as fully threaded screws are prone to damage due to the high frictional force induced during installation [11, 12].

Delahunty, Chui and McCormick [13] applied self-tapping screws to reinforce connections with artificial cracks and confirmed that the reinforcement can improve the load-carrying capacity of cracked connections. However, their work is limited to bolted connections loaded parallel to the grain.

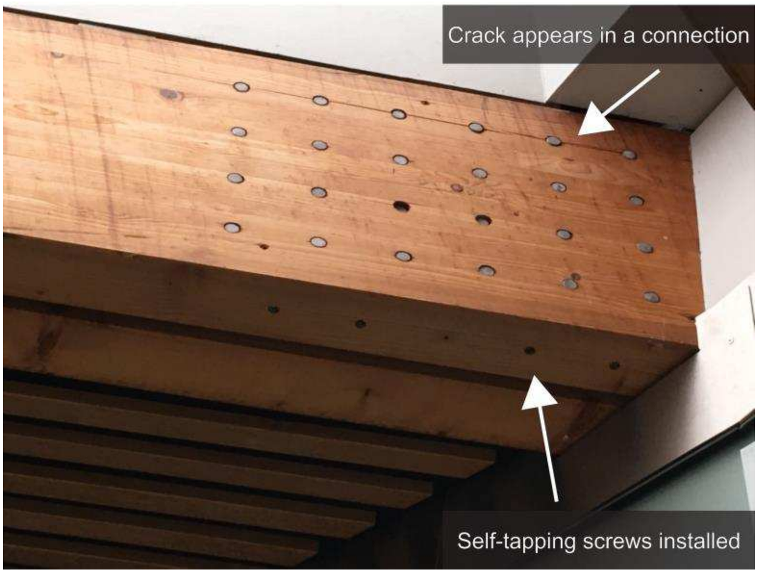

Figure 1: Self-tapping screws are installed from the bottom to repair the connection at the Forum, Exeter.

Currently, there is limited knowledge on using self-tapping screws to reinforce or repair dowel-type moment-resisting connections. Therefore, the purpose of this study is to examine the effectiveness of self-tapping screws with various thread configurations in enhancing the moment resistance of timber connections with and without artificial cracks.

This study also intends to use the embedment properties of wood to predict the moment-resisting capacity of screw reinforced dowel-type connections. There are studies on testing the unreinforced embedment strength of single-dowel connections [14-17] providing mean embedment strength values and only [18] presents both characteristic and mean embedment strength values. In addition, there is limited research focused on the embedment strength of screw reinforcement [19, 20] and their works found that screw reinforcement can enhance the embedment strength of connection. However, their results are presented with mean values. For design purposes, characteristic embedment strength values are used rather than mean values. Therefore, due to limitation in available database, the prediction method proposed by this study used the characteristic embedment strength that were acquired from projects within the scope of this research.

2. Materials and methods

In this study, self-tapping screws were used in dowel-type connections with artificial crack and compared the strength with uncracked connections. The effects of cracks in timber connections were also examined.

Based on previous works [11, 12], this study tends to use self-tapping screws with reduced thread length along their shank. This is practically necessary when long screws are used to reinforce members in large-scale timber structures. The fully threaded screws are vulnerable to damage during installation as large friction forces are generated. Thus, a 300mm long self-tapping screws (Screw X), with 100mm threaded part on the point end, were used to examine the performance of reinforcement.

2.1. Material preparation

The commercial glulam beams in this test were prepared from European Whitewood (Norway spruce (Picea abies) or silver fir (Abies alba)) classified to GL24c. They were conditioned to equilibrium moisture content before and after fabrication (at 21.6℃

temperature and 59% RH). The measured average density is 419kg/m^3 (CoV=3.5%) and average moisture content (M.C.) is 8.4% (CoV=10.0%). A drawing of the screw with flange head is shown in Figure 2 and its detailed specifications and material properties from the technical approval [21] are listed in Table 1.

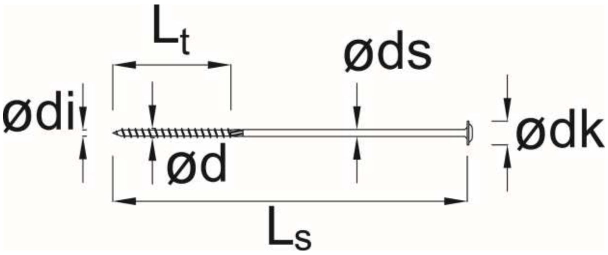

Figure 2: Self-tapping Screw X (8.0mm×300mm) used in this study.

Table 1: Specifications of the self-tapping screw [21].

L_s (mm) Screw length	L_t (mm) Thread length	øds (mm) Shank diameter	ødi (mm) Inner diameter	øds (mm) Outer diameter	ødk (mm) Head diameter
300.00	100.00	8.00	5.30	5.90	20.00
Characteristic yield moment (Nm)			Characteristic tension resistance (kN)		
22.6			8.56		

In this study, the specimen was simplified to one timber member to simulate a timber-steel-timber connection. The span of the glulam beam was 1500mm and was taken to be sufficient to keep the effect of shear deflection in the beam to a negligible value.

Table 2: Summary of each groups

Group	Description	No of tests	Mean density (kg/m^3) (CoV)	Mean M.C.% (CoV)
MCU	Moment Connection Unreinforced	6	419 (6.0%)	7.8 (11.7%)
CMCU	Cracked Moment Connection Unreinforced, 1.5mm crack width	6	419 (2.2%)	8.8 (5.0%)
MCBS	Moment Connection Reinforced by Screw X	6	419 (2.5%)	8.8 (5.5%)
CMCBS	Cracked Moment Connection Reinforced by Screw X, 1.5mm crack width	6	421 (5.4%)	7.8 (15.9%)

In total, 24 tests using 9 glulam beams were conducted and Table 2 lists the details of each group. The specimens for group CMCU were prepared from the tested groups MCU and MCBS using 6 beams (three from each group). One end of the tested beams was cut off and new fastener holes were prepared on the remaining part.

The timber-steel-timber connections consisted of 5mm steel plates slotted into the glulam beam with 67mm thickness on each timber side member. The configuration of the connections was designed according to Eurocode 5 (EC5 hereafter) [22] and the details are shown in Figure 3. The diameter of the dowel was 12mm and a 3×3 fastener group was used for the connections. The steel dowels and steel plates were made from bright mild steel 080A15T and S275, respectively.

The artificial crack was prepared using a bandsaw which had a width of the saw of 1.5mm. The crack was located at the middle row of the dowels and the length was 315mm. A 6mm wide slot was then cut using the bandsaw on both ends of the beam for mounting the 5mm steel plate as the central member. A pre-drilled hole with 5.5mm diameter and 80mm depth was prepared using a pillar drill to ensure the 300mm self-tapping screw could be placed perpendicular to the grain.

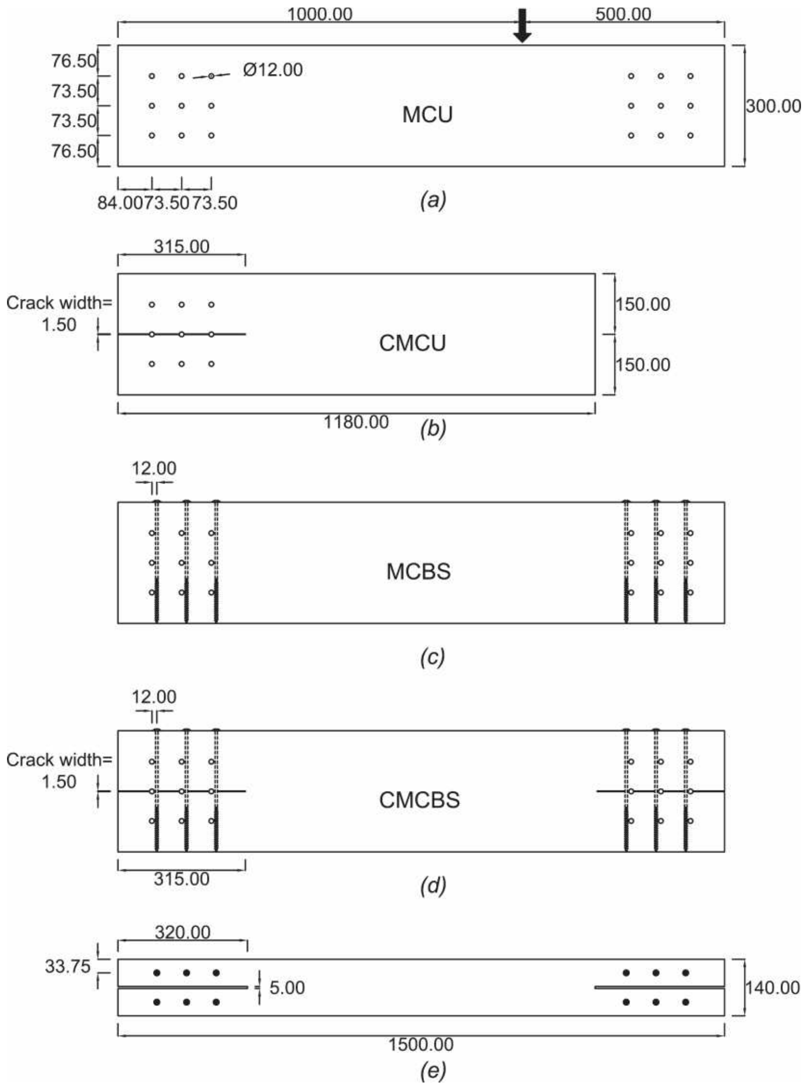

Figure 3: Specimen configurations: (a) Moment Connection Unreinforced (MCU), (b) Cracked Moment Connection Unreinforced (CMCU), (c) Moment Connection Reinforced with Screw (MCBS), (d) Cracked Moment Connection Reinforced with Screw (CMCBS) and (e) top view of the glulam beam indicating the positions of the screw reinforcement.

After fabrication of the specimens, one side of the glulam beam on both ends was painted with black speckle patterns in a matt white background for Digital Image Correlation (DIC). The painted side covered an area of 300mm×315mm where the fastener group was located. DIC was used to track crack propagation and observe surface strain distribution. The painted surface had no difference from the non-DIC side; therefore, cracks could not be controlled to appear on the painted side for analysis.

2.2. Moment-resisting connection test set-up

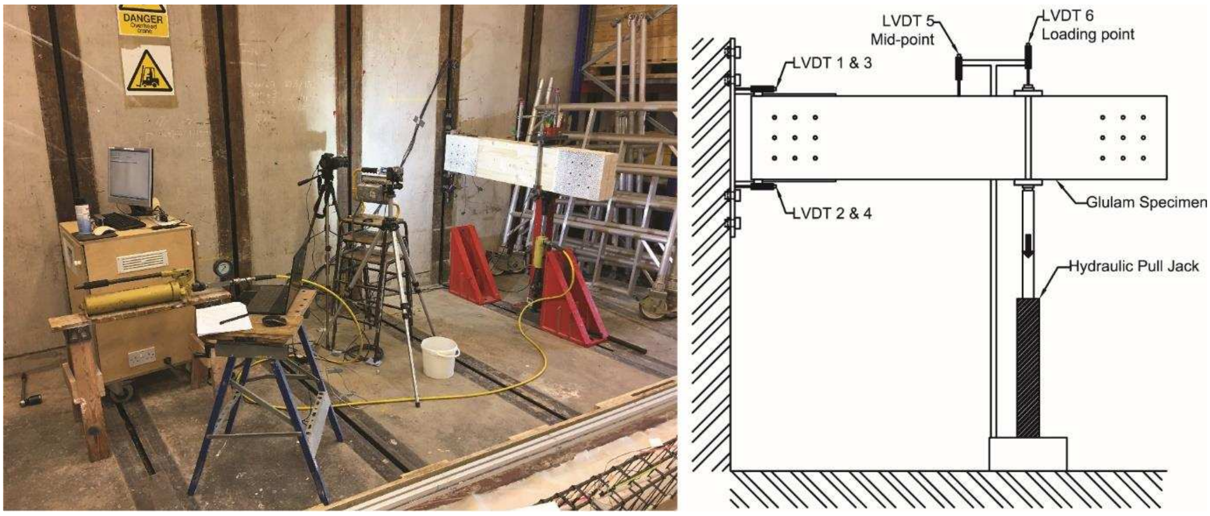

Figure 4: Moment-resisting connection test set-up (left) and locations of the LVDTs (right).

A general view of the test set-up is shown in Figure 4. The glulam beam and the steel plate were placed at 1200mm above the ground and a hydraulic pull jack (with 100kN capacity and 150mm stroke) was bolted to the strong floor in the laboratory. The hydraulic jack pulled the beam downwards 1 metre away from the fixed end and the load was distributed through a steel plate. In this static test, the connection specimens were loaded to failure with around 15-20% load drop from where the peak load was observed. The test was conducted in load-control and at each 0.5kN increment a picture was taken for DIC analysis.

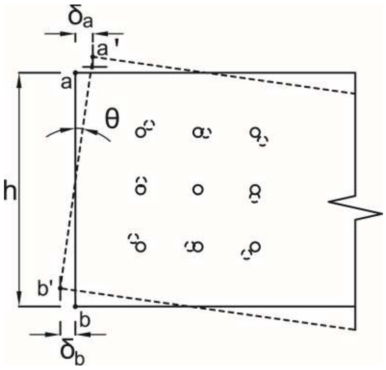

Figure 5: Schematic to measure the rotation of the connections.

A total of 6 linear variable differential transformers (LVDT) (100mm stroke, ±0.01mm accuracy) were deployed in each test and Figure 4 (right) shows their locations. LVDTs 5 and 6 measured the vertical displacement at the mid-point and loading point, respectively. The rotation of the connections is calculated by considering the relative displacement between the LVDT on top and bottom of the beam. As shown in Figure 5, LVDT 1 measured the horizontal displacement from a to *a'* and LVDT 2 gave the measurement from b to b*'*. The angle of rotation of the connections can be calculated as:

$$\theta = arctan\left\{\frac{(a'-a)+(b'-b)}{h}\right\} = arctan\left\{\frac{\delta_a+\delta_b}{h}\right\} \quad (1)$$

where:

h	is the vertical distance between the top and bottom LVDTs and was measured as 335mm in this study;
δ_a and δ_b	are the relative horizontal displacements of the two LVDTs.

3. Results and discussion

3.1. Moment-rotation curves

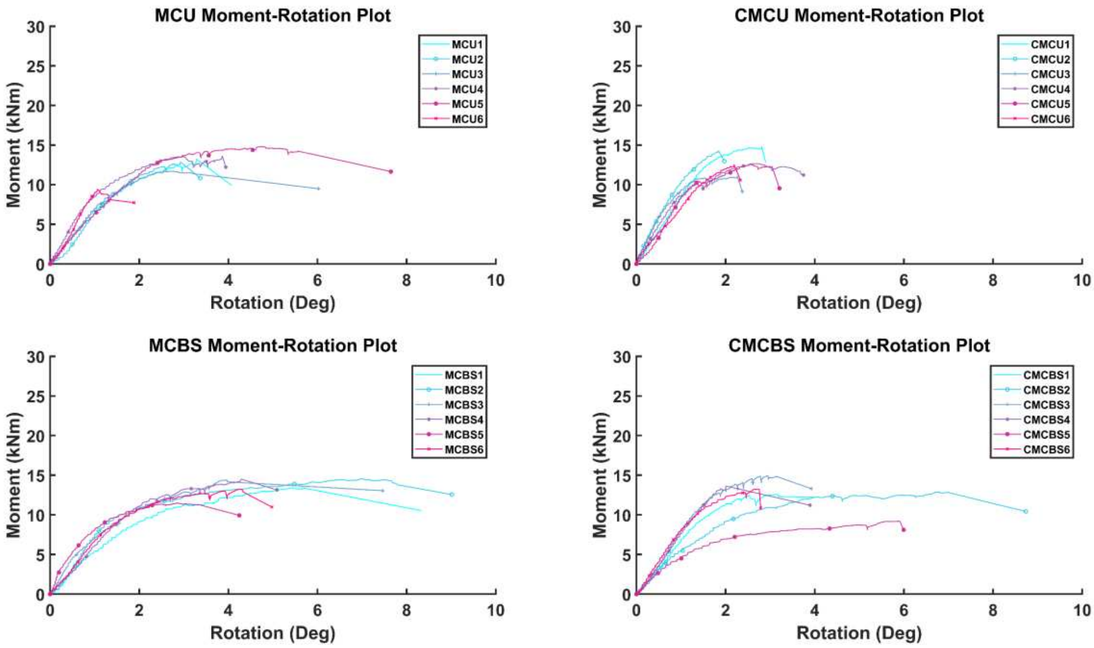

Figure 6: Moment-rotation curves for each group.

Figure 6 demonstrates the moment-rotation curves for the four groups. During the test, the readings of some LVDTs stopped as the stroke on the LVDT was reached or the LVDT stuck due to the movement of the beam. Therefore, to reflect the actual rotational capacity of the connections, the rotation of the connections in the last image from DIC was calculated. A final point can be plotted with the rotation and the corresponding moment. A straight line is drawn between the last available data from the LVDT measurement and the calculated final point. Another method is to use the displacement of LVDT 5 which was placed at the mid-point of the beam. It was used to check the results of the former method. The average percentage difference is found to be 8.9% between the two methods.

As can be seen in Figure 6, even though a similar mean density and variation has been achieved (see Table 2), the connections within a group still display variation in moment-rotation curves. This could result from factors relating to local material defects such as knots.

Table 3 summarises the results of the moment-resisting connection test. The density of connections varies in a range of 398-447kg/m^3 and is considered to have an impact on the test results. A higher density of wood can lead to higher embedment strength and thus a higher moment-resisting capacity. ANCOVA (Analysis of Covariance) is applied to examine the difference between the three groups after effectively removing the influence of density variation.

In terms of moment-resisting capacity, no significant difference was found between the four groups in Table 3. The average capacity of the reinforced group MCBS is about 6.5% higher than the unreinforced group MCU. This implies that partially threaded self-tapping screws can slightly improve the moment-resisting capacity when placed at 1d distance to the dowel. Comparing with group CMCU, it shows that screw reinforcement in group CMCBS did not effectively improve the moment-resisting capacity when the connection was damaged by an artificial crack.

Table 3: Summary of results for each group.

Group	Average moment-resisting capacity (kNm) (CoV) *	Average maximum rotation (°) (CoV) *	Stiffness (kNm per degree) (CoV) *
MCU	13.07 (13%)	4.47 (49%)	9.26 (20%)
CMCU	13.35 (10%)	2.74 (23%)	11.30 (22%)
MCBS	13.92 (8%)	6.51 (31%)	9.18 (26%)
CMCBS	13.35 (15%)	4.95 (44%)	8.28 (25%)

* The values are adjusted by ANCOVA, except the CoV remains for the value before the adjustment.

For the connections designed in this study, a crack due to moisture variation may appear on the top, middle and bottom rows of the fastener group. This study focuses exclusively on connections that have a crack developed at the middle row. Group MCU shows a slightly lower capacity than group CMCU, which has a crack located at the middle row. The result may indicate that a crack located at the middle row may not significantly influence the moment-resisting capacity of a connection. The moment-resisting calculations later in this section also indicate that the middle dowels have the lowest capacity as the force acts perpendicular to the grain (wood with the lowest embedment strength), and they also have the shortest distance to the rotation centre.

For a connection, both the moment-resisting capacity and ductility are important. In this study, the rotational capacity of the connections is considered as an indicator of the ductility of the connections. A crack located at the middle row did not significantly reduce the moment-resisting capacity but it significantly reduced the rotational capacity of the connections which is a crucial factor for designing structures in seismic areas.

In terms of average rotation, the unreinforced group CMCU with artificial cracks showed the lowest value; it had only 61% capacity of the original unreinforced group MCU. This indicates that timber cracking can greatly reduce the rotational capacity of a connection. The reinforced group CMCBS that contained artificial cracks achieved the second-best maximum rotation; it had a capacity even higher than the unreinforced, undamaged ones, by 10.7%. This implies that screw reinforcement can restore the rotational capacity of damaged connections. Finally, the reinforced group MCBS showed the highest rotation, which met expectations, it improved the rotational capacity by 45.6%, when comparing with group MCU. The variation of rotation angle was higher for group MCU and CMCBS which could be a result of the inherent variability of wood materials.

As mentioned in the previous section, the specimens in group CMCU were prepared from the tested beams in groups MCU and MCBS. Specimens CMCU1-3 were prepared from MCU1, 3 and 6, respectively. Using the same beam reduces the variation of material properties due to defects and a comparison of the moment-resisting capacity before and after the application of an artificial crack was made. Overall, it showed an increase of moment-resisting capacity of 13%, 19% and 11% for CMCU1-3 with an artificial crack. Such increase may explain why the group CMCU achieved higher moment-resisting capacity than group MCU. A possible explanation could be due to the local defects, as knots were identified in the glulam beams. After the beams were reused, the fastener groups were located on different locations. Thus, different locations of the fastener group along the beam may have different numbers of defects and the implication is difficult to measure. Therefore, more tests are recommended to minimise the influence of local defects.

For CMCU4-6, the specimens were prepared from group MCBS. However, a similar comparison is not possible with two variables because group CMCU contains artificial cracks without reinforcement while group MCBS contains reinforcement without artificial cracks.

A similar calculation of rotation angle is performed for the connections in groups MCU and CMCU using the same timber beams. An average of 73% of reduction of rotation angle was found when a crack was applied to the middle row. The results provide good correlation to the comparison of the rotation angle between groups MCU and CMCU.

To summarise, self-tapping screws with thread on the point end can slightly improve the moment-resisting capacity and rotational capacity of dowel-type connections when placed at 1d distance from the dowel. It can also restore the rotational capacity of damaged connections to their original status.

3.2. Failure modes

The major failure mode during this test was splitting failure of the beam parallel to the grain and the cracks were mostly located at the top rows of the fasteners group. All of the observed splitting of timber was sudden and accompanied by significant load drop. Table 4 provides a summary of the inspection of each specimen after failure. As the test configuration cannot control the initiation of crack to happen on a specific side, it is difficult to give a detailed observation of the cracks that appeared on the non-DIC side, which had no recording from the DSLR camera or digital video camera. The crack length on the DIC side was measured by the DIC software and for cracks on the non-DIC side, a tape measure was used.

As can be seen in Table 4, the majority of the unreinforced undamaged specimens had splitting on either side of the beam and all the unreinforced specimens with artificial cracks had significant wood splitting. The crack initiated, around the end of the beam and most of the crack propagated either to or beyond the third dowel on the top row. An example of crack propagation in the unreinforced group is shown in Figure 7 (a). The average crack lengths for groups MCU and CMCU were 392mm and 356mm, respectively.

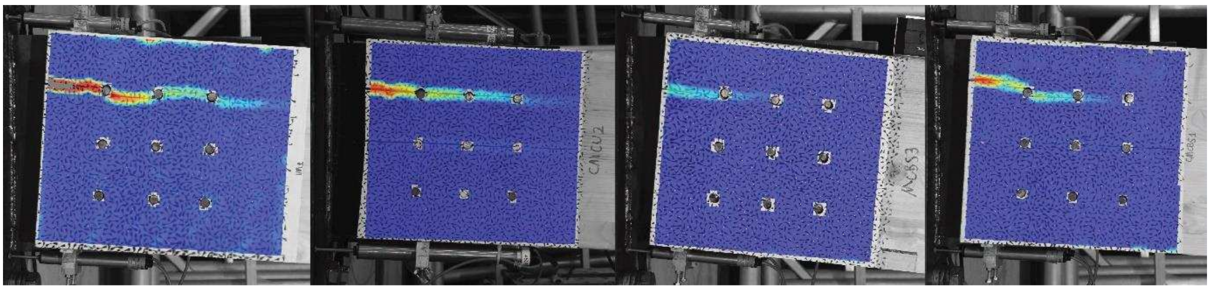

(a) (b) (c) (d)

Figure 7: Observation from DIC on crack propagation at failure point (from left to right): (a) MCU1, (b) CMCU2, (c) MCBS3 and (d) CMCBS1.

In the reinforced group without artificial cracks, only two specimens, MCBS3 and MCBS4, developed a crack on the top row and their cracks reached the second dowel at the point of failure. An example of crack on specimen MCBS3 is shown in Figure 7 (c). The average crack length for group MCBS was 155mm, approximately 60% reduction in length when compared with the unreinforced group MCU.

As for the reinforced specimens with artificial cracks, two of the connections developed new cracks apart from the existing pre-made crack. Their developed cracks reached the third dowel but did not propagate any further at the point of failure, as illustrated in Figure 7 (d). The rest of the group developed no additional cracks and DIC showed stress concentration along the artificial crack, as shown in Figure 8. The stress concentration along the crack was insignificant compared to the crack developed on the top row in Figure 7 (d) and thus was not shown in the image. The average crack length for group CMCBS was 223mm which is 37% shorter than that of the cracked unreinforced group CMCU.

Table 4: A detailed report on specimens after failure.

Specimen	Crack location and longest length on the DIC side	Crack location and longest length on the non-DIC side
MCU1	Top row, 311mm	No crack
MCU2	Top row, 228mm	No crack
MCU3	No crack	No crack
MCU4	Top row, 559mm	No crack
MCU5	Bottom row, 459mm	No crack
MCU6	No crack	Top row, 402mm
CMCU1	No crack	Top row, 227mm
CMCU2	Top row, 353mm	No crack
CMCU3	Top row, 446mm	Top row, 312mm
CMCU4	Top and bottom row, 677mm	Top and bottom row, 617mm
CMCU5	Top and middle row, 273mm	Top and middle row, 246mm
CMCU6	No crack	Top row, 273mm
MCBS1	No crack	No crack
MCBS2	Top row, 159mm	No crack
MCBS3	Top row, 151mm	No crack
MCBS4	No crack	No crack
MCBS5	No crack	No crack
MCBS6	No crack	No crack
CMCBS1	Top row, 229mm; stress concentration on artificial crack	No crack
CMCBS2	Top row, 214mm; stress concentration on artificial crack	Top and bottom row, 221mm
CMCBS3	No crack; stress concentration on artificial crack	No crack
CMCBS4	No crack; stress concentration on artificial crack	No crack
CMCBS5	No crack; stress concentration on artificial crack	No crack
CMCBS6	No crack; stress concentration on artificial crack	No crack

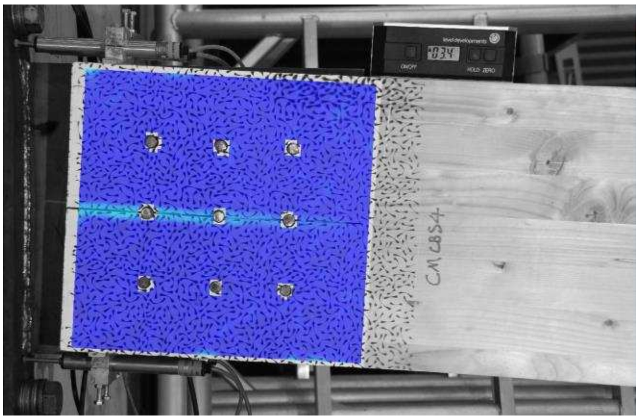

Figure 8: DIC analysis showing stress concentration around the artificial crack at the failure point of specimen CMCBS4.

By comparing the occurrence of splitting failure in the four groups, a preliminary conclusion is that self-tapping screws with partial thread on the point end can reduce the chance of crack initiation and effectively prevent crack propagation in moment-resisting dowel-type connections. The cracks in both reinforced groups show significant reduction in length compared to the unreinforced groups.

Figure 9: Bending of 5mm steel plates (left) and 15mm steel base plate (middle) and yielding of steel dowels (right).

In the test, bending of the steel dowels and steel plates was also observed, as shown in Figure 9. All the dowels except the central one in the moment-resisting connections displayed a level of yielding with a hinge formed at the midpoint of the axial length of the dowels. The yielding of the screw explains the reason for some connections showing load drop without the formation of a crack in Table 4. According to EC5, the failure mode of the connections is mode type 2 which is a combination of embedment failure and single yield failure of the fastener.

However, none of the self-tapping screws used in this study displayed significant screw head embedment into the wood as shown in Figure 10. In previous studies [11, 12], screw head embedment is a result of a combination of bending of the screw and the action to split the wood by tensile load perpendicular to the grain. The self-tapping screws were retrieved after the test while visual observation does not identify significant damage to the screws.

Figure 10: The specimen from MCBS5 shows no sign of screw head embedment after the test.

One possible explanation is that some dowels were not in contact with the screw at the point of failure, because the self-tapping screws were placed at 1d (≈ 12mm) distance from the dowel. The purpose of a 1d spacing was to avoid the risk of the screw passing through the holes for the fasteners due to the existence of knots that may have caused the screw to deviate from its original vertical course during installation. The action of bending of the screw was not possible, thus, the embedment of the screw head was insignificant. The connection part of MCBS2 was cut off from the beam and a band saw was used to separate the part into two for inspection. In Figure 11, it is observed that, as suggested above, the dowels were not in contact with the screws by the point of failure of the connection.

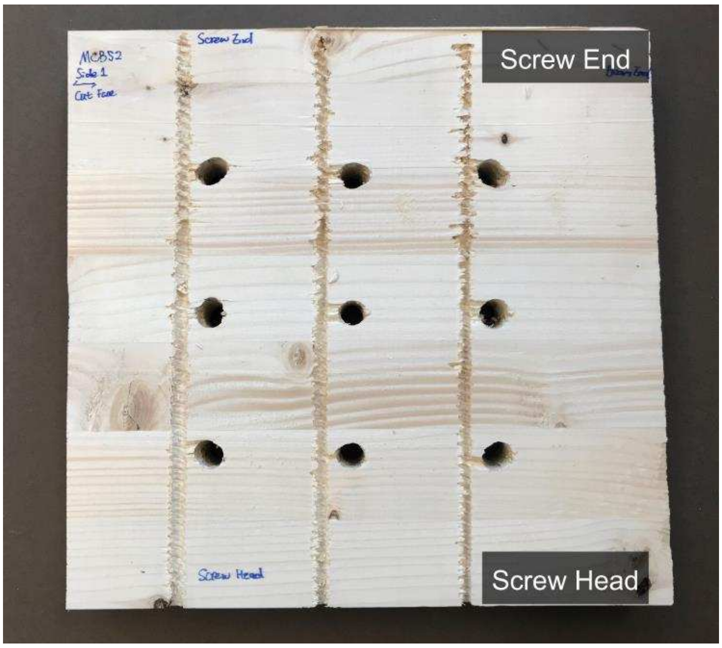

Figure 11: Inspection of screw and dowel interaction in the connection area in group MCBS2.

Therefore, the tendency for screw head embedment mainly depends on the splitting action of wood. However, as recorded in Table 4, the reinforced connections showed no significant cracking, indicating that the splitting action is also reduced. This implies that self-tapping screws as reinforcement can effectively control crack propagation as a higher rotational capacity is found in the reinforced groups in Table 3.

4. Theoretical prediction of moment-resisting capacity of dowel-type connections

Currently, the industry is promoting the use of glulam products and proposing large-scale, high-rise timber buildings. Studies have indicated that self-tapping screws are effective as reinforcement and also possess the advantage of simplicity, as they are easy to install and require less space than steel or FRP reinforcement. On the other hand, there is no guidance given in standards to calculate the moment-resisting capacity of dowel-type connections reinforced by self-tapping screws. Therefore, this study proposes a method to calculate the moment-resisting capacity of screw-reinforced dowel-type connections.

4.1. Assumption and procedures

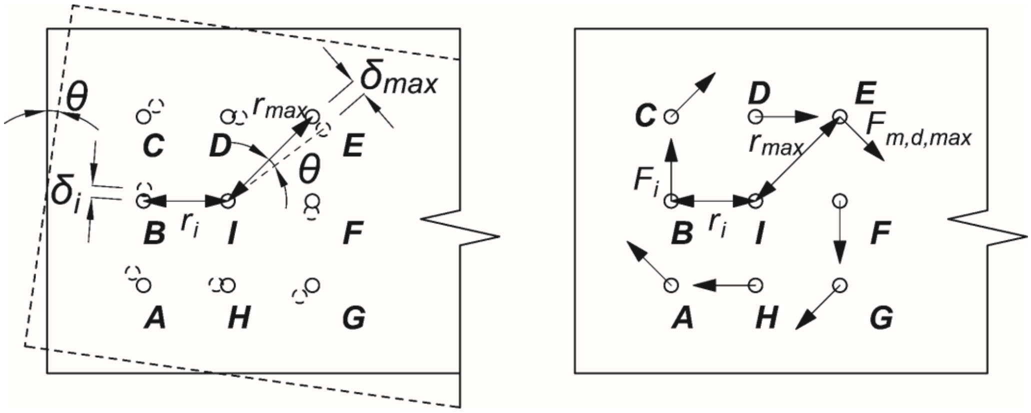

Figure 12: The rotational behaviour of the fasteners in the tested specimen.

Key points of the proposed prediction method are summarised in the following paragraphs.

The connection is regarded as rotationally rigid. For a rigid model, one important assumption is that the centre of rotation remains fixed under loading. In addition, the centre of rotation is taken as the centre of the fastener group and all the fasteners are applied with the same linear-stiffness behaviour in the analysis. Figure 12 shows the rotation of fasteners around the centre at angle, θ, and transfer loads normal to the direct distance from the centre.

The method is based on the calculation model that was demonstrated in Blaß [23] and Porteous and Kermani [24] for a rotationally rigid connection:

$$M_d = (\frac{F_{m,d,max}}{r_{max}} \sum_{i=1}^{n} r_i^2) \cdot n_{sp} \quad (2)$$

where:

M_d is the design moment-resisting capacity of the connections;

$F_{m,d,max}$ is the maximum load normal to its distance to the centre of rotation due to the moment imposed on the connections;

r_{max} is the maximum distance between the dowel and the centre of rotation;

n is the number of dowels;

i represents the dowel in the connections;

r_i is the distance between the dowel and the centre of rotation;

n_{sp} is the number of shear planes.

In the experimental tests of this study, mode type 2 failure (including the embedment failure of wood and single yield failure of the dowel) was observed. For convenience, the labels for the dowels are used to represent the area where mode type 2 failure has occurred. For instance, '*failure of Area A'* indicates that dowel A and the wood around it has failed.

In the proposed method, the vertical load, F, acting on the beam is considered into calculation. With the additional vertical load, the angle of the total load on the dowel to the grain direction is changed and the corresponding embedment strength can be different, leading to various $F_{m,d,max}$ and M_d, for the dowels furthest from the centre of rotation (e.g. dowels A and C comparing to dowels E and G in Figure 13 (b) in the next section). Therefore, the fastener areas may not fail simultaneously even though they have same direct distance to the centre of rotation, as the local mechanical properties are influenced by the loading direction, reinforcement and artificial damage.

Thus, the fundamental idea of the proposed method is to input the characteristic embedment strength from previous study [11] (listed in Table 5) to predict the $F_{m,k,max}$ and M_k based on the loading condition of each dowel. Then, finding the sequence of failure of the areas by sorting the acquired M_k values from the smallest to the largest. Finally, calculating the characteristic moment-resisting capacity of the connections by considering the early failure of certain areas.

The proposed method estimates the moment-resisting capacity at ultimate load. Due to the nature of the reinforcement method, not all the fasteners are bearing on the reinforced wood. Some of the fasteners are bearing on unreinforced wood leading to a lower load-carrying capacity and that area around it would tend to fail earlier than those having fasteners bearing on reinforced wood. It is less accurate to use the load-carrying capacity, which is calculated based on the condition that the fastener is bearing on unreinforced wood, to predict the moment-resisting capacity of the reinforced connections. In this case, an assumption is made that the connection is effective until failure has occurred to three or four fastener areas, and the failed areas continue to provide their full load-carrying capacity and support to vertical load until the total number of failed areas reaches to 3 or 4 (involving at least one failure area that is reinforced). This is done in order to include the reinforcement effect when calculating the capacity of reinforced connections. To ensure consistency, this assumption is applied to all types of connections tested in this study.

It is proposed that the criteria to consider failure of reinforced connections is the prediction must involve the failure of at least one reinforced area.

Furthermore, this study assumes the vertical load on the dowels is evenly distributed. In a real connection, there is a lack of fit of the dowels (gaps around the dowels) at the beginning and the gaps close as the dowels take up load progressively. Therefore, the prediction in this study is based on the situation after initial rotation has closed the gaps around the dowels.

The characteristic moment-resisting capacity of the four types of connections are given in Table 6 and a demonstration of calculation is shown for the reinforced connections without crack.

4.2. Reinforced connections MCBS

The perpendicular distance L of the vertical load, F, to the centre of rotation of the connections is 842.5mm and the load is equally divided into nine components acting on the fasteners by two shear planes with each denoted as, F_v, as shown in Figure 13. The forces on the dowels due to the moment, M, are denoted as, F_X. The total forces acting on the dowels are represented by F_{TX} and their angles to the grain direction are represented by α_{TX} as demonstrated in Figure 13 (b) where X is the letter representing the dowel as shown in Figure 13. The direction of the total force on each dowel is different depending on the combination of the imposed loads. The maximum and minimum perpendicular distances from a fastener to the centre of rotation are 103.94mm (r_{max}) and 73.50mm (r_i), respectively.

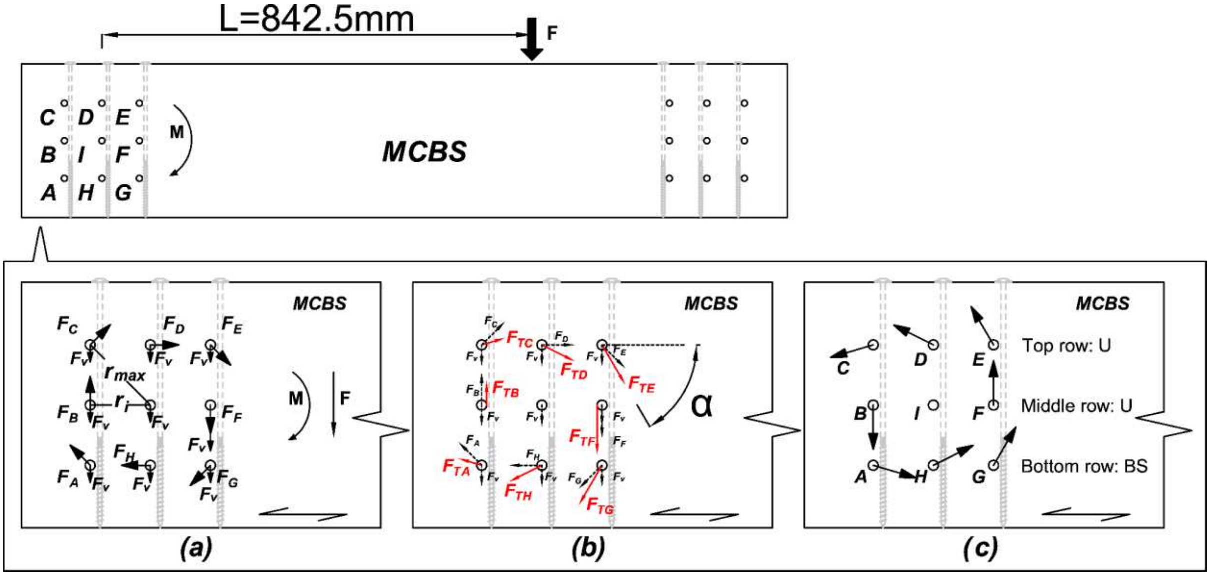

Figure 13: Forces and their directions on each dowel in group MCBS: (a) vertical load F_V and load due to rotation F_X imposed on each dowel; (b) total load F_{TX} and its direction α_{TX}; (c) the relative direction of movement of the dowels due to rotation.

Based on the demonstration in Figure 13, it can be found that dowels E and G are the critical points as they sustain the highest total load, which is a combination of the load due to moment and the vertical load. However, as indicated in Figure 13 (c), the relative movement of the dowels is anti-clockwise. Thus, only dowels A, H and G are bearing on screw reinforced wood with a higher embedment strength and a higher load-carrying capacity. Therefore, it is assumed that failure occurs to Area E first.

The moment-resisting capacity of the connections, M_k can be expressed as:

$$M_k = FL = [(F_A + F_C + F_E + F_G) \cdot r_{max} + (F_B + F_D + F_F + F_H) \cdot r_i] \cdot n_{sp} \quad (3)$$

where:

F is the vertical load acting on the beam in Figure 13;

L is the perpendicular distance of the vertical load, F, to the centre of rotation of the connections and is measured to be 842.5mm in this study;

r_{max} is the distance from the centre of the fastener group to the furthest fastener;

r_i is the distance from the centre of the fastener group to the furthest fastener;

n_{sp} is the number of shear planes.

In this study, a moment acting on the connection causes a rotation of θ and a displacement of δ_{max} in dowel E as shown in Figure 14. The load on the dowel due to the rotation is the product of the slip modulus and the displacement. For a rigid model, the dowels with equal perpendicular distance, either r_{max} or r_i, to the centre of rotation are subject to the same amount of load assuming they have same slip modulus, K, and rotation angle, θ. Thus:

$$F_A = F_C = F_E = F_G = K \cdot \delta_{max} = K \cdot r_{max} \cdot \theta \quad (4)$$

$$F_B = F_D = F_F = F_H = K \cdot \delta_i = K \cdot r_i \cdot \theta \quad (5)$$

where:

K is the slip modulus for each fastener and assumed to be a constant in here;

δ is the displacement of the fastener;

θ is the rotation of the connection.

The force F_E, acting on dowel E is under consideration in this step. The forces on dowels B, D, F and H are the same and their magnitude can be found by knowing the proportion between r_{max} and r_i based on equations (4) and (5), therefore:

$$F_B = F_D = F_F = F_H = \frac{F_E}{r_{max}} \cdot r_i \quad (6)$$

The loads on dowels A, C, E and G are the same and substituting the load on each fastener in relation to the load on dowel E into Equation (3), the equation to calculate the characteristic moment-resisting capacity of the connections can be simplified and expressed as:

$$M_k = FL = (4F_E \cdot r_{max} + 4\frac{F_E}{r_{max}} \cdot r_i^2) \cdot n_{sp} \quad (7)$$

Rearranging the equation:

$$F_E = \frac{FL}{4n_{sp}} \cdot \frac{1}{(r_{max} + \frac{r_i^2}{r_{max}})} \quad (8)$$

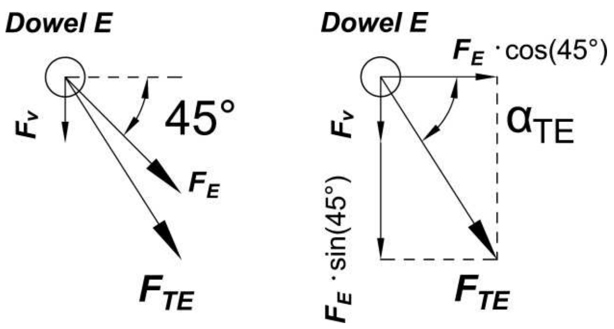

Figure 14: (a) The loads acting on dowel E; (b) Resolving the loads into vertical and horizontal components.

As shown in Figure 14 (b), the magnitude and angle of the total load on dowel E, F_{TE}, can be found by resolving F_v and F_E into horizontal and vertical components. The load due to moment, F_E, is at 45° to the horizontal direction. The load in the vertical direction is the sum of the F_v and the components of F_E:

$$F_{vertical} = F_v + F_E \cdot sin(45°) = \frac{F}{n_{sp}n} + F_E \cdot sin(45°) = \frac{F}{2\times9} + \frac{\sqrt{2}}{2}F_E = \frac{F}{18} + \frac{\sqrt{2}}{2}F_E \quad (9)$$

where:

F_v is the vertical load on the fastener;

F_E is the load on the fastener due to moment;

F is the vertical load on the connection;

n_{sp} is the number of shear planes;

n is the number of fasteners.

The horizontal component is contributed from the load F_E only. Therefore, the following equation can be established:

$$tan(\alpha_{TE}) = \frac{(\frac{F}{18}+\frac{\sqrt{2}}{2}F_E)}{\frac{\sqrt{2}}{2}F_E} \quad (10)$$

By substituting Equation (8) and the values for L, n_{sp}, r_{max} and r_i into Equation (10), the angle of F_{TE} to the grain direction, α_{TE} is:

$$\alpha_{TE} = tan^{-1}\left[1 + \frac{8\sqrt{2}}{18L}\cdot(r_{max} + \frac{r_i^2}{r_{max}})\right] = 48.15° \quad (11)$$

Thus, the total load on the dowel F_{TE} should not exceed the load-carrying capacity in this direction. The load-carrying capacity can be calculated using the following equations from EC5 [22]:

$$F_{v,Rk} = min\begin{cases} f_{h,1,k}t_1 d & (f) \\ f_{h,1,k}t_1 d\left[\sqrt{2 + \frac{4M_{y,Rk}}{f_{h,1,k}dt_1^2}} - 1\right] + \frac{F_{ax,Rk}}{4} & (g) \\ 2.3\sqrt{M_{y,Rk}f_{h,1,k}d} + \frac{F_{ax,Rk}}{4} & (h) \end{cases} \quad (12)$$

where:

$f_{h,1,k}$ is the characteristic embedment strength in the timber member;

t_1 is the smaller of the thicknesses of the timber side member or the penetration depth;

d is the fastener diameter;

$M_{y,Rk}$ is the characteristic fastener yield moment;

$F_{ax,Rk}$ is the characteristic withdrawal capacity of the fastener and is equal to zero for steel dowels.

$F_{v,Rk}$ depends on the characteristic embedment strength of the wood, $f_{h,1,k}$, in the loaded angle, α_{TE}, to the grain direction and in here is 0°, 45° and 90° as shown in Figure 12. Based on the characteristic embedment strength parallel to the grain, $f_{h,0,k}$, acquired from [11], as shown in Table 5, $f_{h,1,k}$, can be calculated through the Hankinson formula given in clause 8.5.1.1 (2) in EC5:

$$f_{h,\alpha,k} = \frac{f_{h,0,k}}{k_{90}sin^2\alpha + cos^2\alpha} \quad (13)$$

where:

k_{90} is equal to 1.53 for a member made of softwood and connected by 12mm diameter dowels.

The embedment tests from Table 5 were acquired from previous tests of European Whitewood using 16mm dowels with same material properties for the 12mm dowels used in this study. The loading direction of the embedment test was parallel to the grain.

Table 5: Summary of characteristic values calculated based on previous test [11].

Group	Description	Characteristic embedment strength from previous test, $f_{h,0,k}$ (N/mm^2)
U	No crack, unreinforced	20.07
BS	No crack, reinforced by screw with 33% thread on the point end	24.80
C1.5U	1.5mm crack, unreinforced	14.91

As mentioned previously, the wood that dowel E is bearing on is unreinforced due to the relative movement of the dowel during rotation; and, for a connection with dowel E, the load-carrying capacity can be found by using the unreinforced embedment strength (U) at 48.15˚ to the grain direction. For unreinforced wood, if no reference values are available from tests, the use of the formulas in EC5 Equation 8.31 is recommended to calculate the characteristic embedment strength. Another approach is to acquire the embedment strength experimentally following BS EN 383:2007 [25] and using BS EN 14358:2016 [26] to calculate the characteristic value.

There is other available literature that presents values of embedment strength of unreinforced and screw-reinforced wood in [14-20]. However, most of the available results are not characteristic values but mean values.

Thus, from Equation (12), $F_{v,Rk}$ is calculated to be 6.74kN (mode type 2 failure) and F_{TE} is not greater than this value. As the horizontal component of F_{TE} is contributed by F_E (see Figure 14), a relationship between F_{TE} and F_E is demonstrated below:

$$F_{TE} \cdot cos(48.15^{\circ}) = \frac{\sqrt{2}}{2} F_E \tag{14}$$

Therefore, F_E equals to 6.36kN when the maximum value of 6.74kN is assigned to F_{TE}. Substituting the value of F_E into Equation (7), the characteristic moment-resisting capacity of the reinforced connections based on the load-carrying capacity of a connection contains dowel E is found to be 7.93kNm.

By this point, only one area has failed and the prediction does not consider the enhancement of embedment strength due to the screw reinforcement. Therefore, the predicted value is not accurate enough for a reinforced connection. As previously mentioned, the failed area will still provide the load-carrying capacity and vertical support until two or three more areas fail. The ultimate state of the connections has not yet been reached.

To have a more accurate prediction, the capacity of the reinforced connections is checked regarding to Areas C, F and G, respectively, based on the failure of Area E (a combination of embedment failure and fastener failure). The connections are likely to fail at these locations with a higher total load (see Figure 13 (b)). A new equation is established based on the load on dowel C (F_C is equal to F_A) for demonstration:

$$M_k = FL = (3F_C \cdot r_{max} + 4\frac{F_C}{r_{max}} \cdot r_i^2 + F_E \cdot r_{max}) \cdot n_{sp} \quad (15)$$

Rearranging the equation:

$$F_C = \frac{FL - F_E \cdot r_{max} \cdot n_{sp}}{(3 \cdot r_{max} + 4 \cdot \frac{r_i^2}{r_{max}}) \cdot n_{sp}} \quad (16)$$

The above equation can be represented by:

$$F_C = xF - y \quad (17)$$

Substituting the constants and the values for F_E from the previous calculation into the expressions:

$$x = \frac{L}{(3 \cdot r_{max} + 4 \cdot \frac{r_i^2}{r_{max}}) \cdot n_{sp}} = 0.81 \qquad y = \frac{F_E \cdot r_{max} \cdot n_{sp}}{(3 \cdot r_{max} + 4 \cdot \frac{r_i^2}{r_{max}}) \cdot n_{sp}} = 1.27 \quad (18)$$

$$\therefore F_C = 0.81F - 1.27 \quad (19)$$

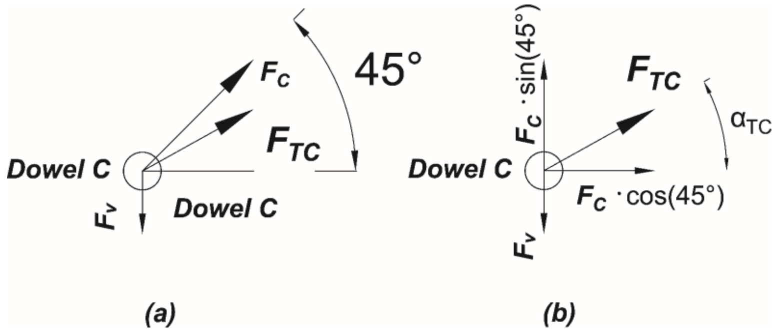

Figure 15: (a) The loads acting on dowel C; (b) Resolving the loads into vertical and horizontal components

The angle between the total load on dowel C and the grain direction, α_{TC}, is assumed to be the angle when failure occurs to Area E. Unlike the expression in equation (10), the load F_C, due to moment acting on dowel C, is in the opposite direction to the vertical load F_v, see Figure 13 (b) and Figure 15 (a). Therefore, the relationship between α_{TC} and the horizontal and vertical components of F_{TC} is now:

$$tan(\alpha_{TC}) = \frac{\left(\frac{\sqrt{2}}{2}F_C - \frac{F}{18}\right)}{\frac{\sqrt{2}}{2}F_C} = 1 - \frac{F}{18} \cdot \frac{\sqrt{2}}{F_C} \quad (20)$$

The corresponding load F_C on dowel C at that moment can be found using the relationship identified in Equation (4). Dowels C and E have the same distance to the centre of rotation r_{max}, slip modulus K and rotation angle θ:

$$F_C = \frac{K \cdot r_{max} \cdot \theta}{K \cdot r_{max} \cdot \theta} F_E \quad (21)$$

The vertical load F_v on dowel C at that moment is the vertical load F on the beam divided by 18 (with nine dowels and two shear planes) (when dowel E has failed) and is calculated to be 0.52kN (from previous calculation on dowel E). Thus, the angle of the total load on dowel C can be found by substituting Equation (21) into Equation (20) and knowing the value of load FE also from previous calculation on dowel E:

$$\alpha_{TC} = tan^{-1}\left[\frac{\left(\frac{\sqrt{2}K \cdot r_{max} \cdot \theta}{2\ K \cdot r_{max} \cdot \theta}F_E - \frac{F}{18}\right)}{\frac{\sqrt{2}K \cdot r_{max} \cdot \theta}{2\ K \cdot r_{max} \cdot \theta}F_E}\right] = tan^{-1}(1 - \frac{F}{18} \cdot \frac{\sqrt{2}}{F_E}) = 41.47° \quad (22)$$

Dowel C will move away from the self-tapping screw (see Figure 13 (c)), meaning that the wood it bears on is not reinforced. Thus, the embedment strength is taken for the unreinforced value (U) in Table 5 at 41.47˚ to the grain direction using the Hankinson formula (Equation (13)). The embedment strength is then substituting into the load-carrying capacity equations for a connection (Equation (12)). Therefore, the load-carrying capacity of a connection contains dowel C can be found as 7.01kN and the total load F_{TC} cannot be greater than this value.

For dowel C, a relationship between the total load F_{TC}, the load F_C due to the moment and the vertical load F_v can be established (see Figure 15 (b)):

$$F_{TC}^2 = (\frac{\sqrt{2}}{2}F_C)^2 + (\frac{\sqrt{2}}{2}F_C - \frac{F}{18})^2 \qquad (23)$$

Substituting Equation (19) into Equation (23), a quadratic equation with unknown F can be written as following:

$$0 = (x^2 - \frac{x\sqrt{2}}{18} + \frac{1}{324})F^2 + (-2xy + \frac{y\sqrt{2}}{18})F + (y^2 - F_{TC}^2) \qquad (24)$$

Where F_{TC} can be found using Equations (12) and (13) and the above equation can be solved which gives the values of F to be 10.72 or -7.43. The value of the load F is taken to be the positive solution of the quadratic equation. The characteristic moment-resisting capacity of the reinforced connections at the ultimate state is the product of the load on the beam (F) and the perpendicular distance of load to the centre of rotation (L) and is calculated to be 9.03kNm.

Using the same method for Area C, the characteristic moment-resisting capacity of the connections can be found when Areas F (at 9.15kNm) and G (at 9.17kNm) fail respectively, with prior failure to Area E. With a higher moment-resisting capacity than 9.03kNm, it implies that areas fail in a sequence of E, C, F and G.

The next step is to find the moment-resisting capacity of the connections when Area F fails with Areas E and C having already failed. Similarly, an equation can be established as follows:

$$M_k = FL = (2F_F \cdot r_{max} + 4\frac{F_F}{r_{max}} \cdot r_i^2 + F_E \cdot r_{max} + F_C \cdot r_{max}) \cdot n_{sp} \qquad (25)$$

Repeating the above steps and using the unreinforced embedment strength (U) for the wood around dowel F, the characteristic moment-resisting capacity of the connections when Areas E, C and F have failed is 9.13kNm. As can be seen, the moment-resisting capacity has increased 16% from the first failure of Area E. However, the additional capacity due to the enhanced embedment strength from reinforcement is not considered as the wood around dowels E, C and F is unreinforced due to the movement of the dowels.

Thus, the final step is to calculate the moment-resisting capacity of the connections based on Area G with Areas E, C and F having failed already. Another equation is established:

$$M_k = FL = (2F_G \cdot r_{max} + 3\frac{F_G}{r_{max}} \cdot r_i^2 + F_E \cdot r_{max} + F_C \cdot r_{max} + F_F \cdot r_i) \cdot n_{sp} \qquad (26)$$

The wood around dowel G is assumed to be reinforced with an enhanced embedment strength calculated from (BS) in Table 5 and the final characteristic moment-resisting capacity of the reinforced connections MCBS is found to be 9.14kNm.

4.3. Predicted values for characteristic moment-resisting capacity

Table 6: Summary of predicted values for the connections in this study and brief details for each calculation steps.

	Step	Calculation based on dowel	Early failure of area	Embedment strength based on previous study	Total load to grain angle α	Load on the early failed dowel (kN)	Moment-resisting capacity (kNm)
MCU	1	E (G) *	N/A	U	48.15˚	N/A	7.93
	2	C (A) *	N/A	U	41.47˚	N/A	9.27
	3	C (A) *	E & G	U	41.47˚	F_E=6.36	8.80
		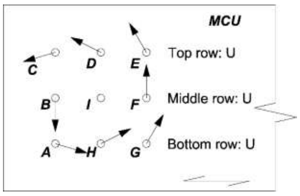		$M_k = FL = (2F_C \cdot r_{max} + 4\frac{F_C}{r_{max}} \cdot r_i^2 + F_E \cdot r_{max} + F_G \cdot r_{max}) \cdot n_{sp}$			
CMCU	1	F	N/A	C1.5U	90.00˚	N/A	7.55
	2	E (G) *	F	U	48.15˚	F_F=4.28	7.90
		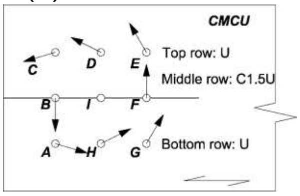		$M_k = FL = (4F_E \cdot r_{max} + 3\frac{F_E}{r_{max}} \cdot r_i^2 + F_F \cdot r_i) \cdot n_{sp}$			
MCBS	1	E	N/A	U	48.15˚	N/A	7.93
	2	G	E	BS	48.15˚	F_E=6.36	9.17
	3	F	E	U	90.00˚	F_E=6.36	9.15
	4	C	E	U	41.47˚	F_E=6.36	9.03
	5	F	E & C	U	90.00˚	F_E=6.36, F_C=7.42	9.13
	6	G	E, C & F	BS	48.15˚	F_E=6.36, F_C=7.42, F_F=5.33	9.14
		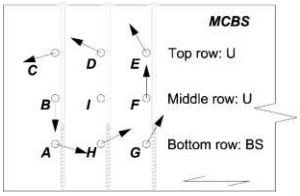		$M_k = FL = (2F_G \cdot r_{max} + 3\frac{F_G}{r_{max}} \cdot r_i^2 + F_E \cdot r_{max} + F_C \cdot r_{max} + F_F \cdot r_i) \cdot n_{sp}$			
CMCBS	1	F	N/A	C1.5U	90.00˚	N/A	7.55
	2	E	F	U	48.15˚	F_F=4.28	7.90
	3	C	F & E	U	41.47˚	F_F=4.28, F_E=6.36	8.88
	4	G	F & E	BS	48.15˚	F_F=4.28, F_E=6.36	9.02
	5	G	F, E & C	BS	48.15˚	F_F=4.28, F_E=6.36, F_C=7.40,	8.99
		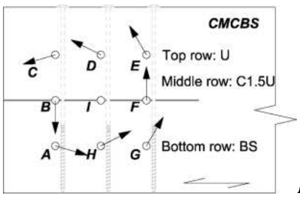		$M_k = FL = (2F_G \cdot r_{max} + 3\frac{F_G}{r_{max}} \cdot r_i^2 + F_E \cdot r_{max} + F_C \cdot r_{max} + F_F \cdot r_i) \cdot n_{sp}$			

* Dowel in the brackets fail simultaneously.

Table 6 lists the calculation steps for each group tested in this study. In groups CMCU and CMCBS, the dowels B and F will tend to move parallel to the grain direction and a crack passes through the dowels. Therefore, cracked unreinforced embedment strength of wood (C1.5U) from Table 5 is used.

Table 7 summarises the predicted capacity compared with the characteristic moment-resisting capacity from the connection tests. The characteristic moment-resisting capacity from the connection tests is calculated according to the 5-percentile method in BS EN 14358:2016 [26].

As can be seen from Table 7, the calculation method gives underestimated values when compared to the characteristic values calculated from the test which is in line with expectation that prediction should provide a conservative value. Comparing the calculated characteristic values with the predicted values, the unreinforced group MCU shows a 5% difference. This implies that the method is conservative but is still an accurate estimation of the moment-resisting capacity of the connections. As for the other three groups, the prediction method is also conservative but with a higher percentage error. The proposed method is based on the existing method which does not consider the influence of crack and reinforcement. Applying the embedment strength for each different situation in the proposed method would gain a more accurate estimation but the reduction of the percentage error requires further investigation and modification of the method. The proposed method provides an insight into predicting the moment-resisting capacity of screw-reinforced dowel-type connections.

Table 7: Calculated characteristic moment-resisting capacity from tests and estimated characteristic moment-resisting capacity based on proposed calculation method.

	MCU	CMCU	MCBS	CMCBS
Characteristic moment-resisting capacity calculated based on six repetitions (kNm)	9.26	10.41	12.94	12.06
Characteristic moment-resisting capacity of connections estimated by using the characteristic value of embedment tests (kNm)	8.80	7.90	9.14	8.99
Percentage error between the characteristic test and predicted values	5.0%	24.1%	29.4%	25.5%

As screw reinforcement involves strengthening the wood material, it has been assumed that such reinforcement could change the basic assumption that all the steel dowels rotate around the centre of the fastener group. To further validate the credibility of the proposed modes, DIC analysis was used to identify the movement of fasteners under certain rotations of the connections. Specimen rotation at 2.5˚ was chosen and the corresponding images were selected. DIC analysis can show the horizontal and vertical displacement of points around the dowels on the images and the movement of the dowels (displacement and direction) can be calculated. This method helps to demonstrate whether the fasteners in the reinforced specimens rotate around the centre of rotation, as illustrated in Figure 12.

The result is shown in Figure 16 with the theoretical rotation direction of the dowels represented by a solid line with an arrow. The actual rotation direction of the dowel is represented by a dashed line. The theoretical displacement can be found by calculating the distances between the dowels and the centre of rotation but is not displayed in Figure 16. Overall, the realistic movement of the fastener in all specimens showed good correlation to theoretical movement in both displacement and rotation. Therefore, it confirms that specimens reinforced by self-tapping screws placed at 1d fastener spacing follows the assumption that all fasteners rotate around the centre of the fastener group and validates the proposed method for calculating the moment-resisting capacity of reinforced dowel-type connections.

Furthermore, DIC analysis calculated the displacement of the centre dowel as shown in Figure 16. The values of displacement for all four groups are small and negligible. This confirms the previous assumption that the centre of the fastener group remains fixed. The displacements of the centre dowels at smaller theoretical and measured rotation (e.g. 1° and 2°) are not shown in this study, while their values are also found to be small.

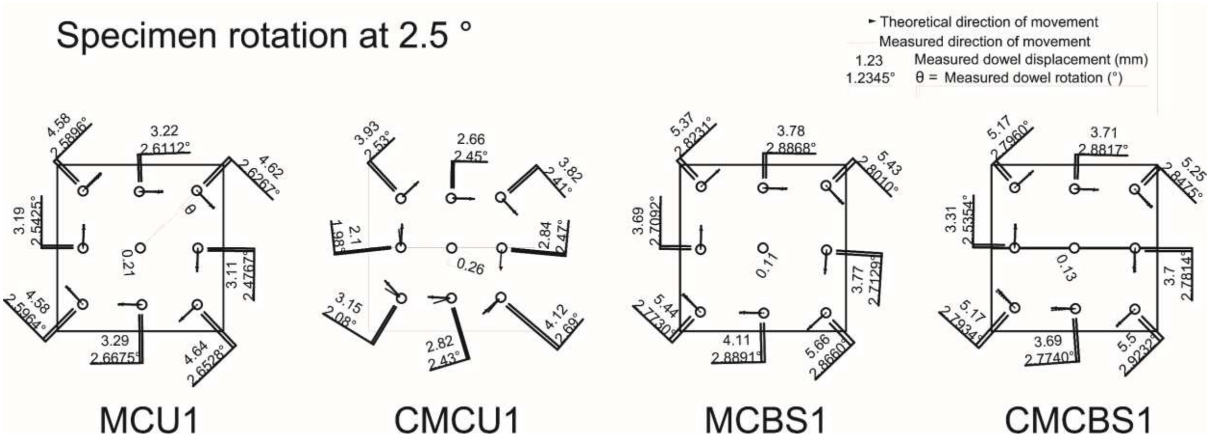

Figure 16: Measured dowel displacement at 2.5° rotation angle. Most of the dashed lines representing the actual direction are hardly visible due to the high correlation with the theoretical direction.

5. Conclusion

This study investigates the performance of dowel-type moment-resisting connections reinforced by self-tapping screws compared with unreinforced connections. Enhancement of screw reinforcement on artificially damaged connections is also investigated. The following points can be concluded from the results in this study:

- Partially threaded self-tapping screws placed at one fastener spacing to the dowel can enhance rotational capacity while the improvement in moment-resisting capacity is slight.
- When a connection was damaged by making a 1.5mm artificial crack at the middle row of its fastener group, self-tapping screws as reinforcement restored the rotational capacity to its original undamaged state.
- Based on experimental observation, the tendency of splitting failure was greatly controlled by the application of self-tapping screws. In addition, according to images from DIC, crack propagation was also controlled by having self-tapping screws. The average crack lengths in the unreinforced groups MCU and CMCU were 392mm and 356mm, respectively. The average crack lengths in the reinforced groups MCBS and CMCBS were 155mm and 223mm, respectively. The average crack length in reinforced specimens was at least 37% shorter than in the unreinforced ones.
- A calculation method for predicting the moment-resisting capacity of connections reinforced by screws is proposed and shows conservative values when compared with experimental results (percentage error ranging from 5-29.4%). The displacement results from DIC also validated that the steel dowels in the reinforced specimen followed the assumption that they rotate around the centre of the fastener group. Therefore, the proposed method can be used to predict the moment-resisting

capacity of screw reinforced dowel-type connections with similar configuration of connections and screw reinforcement.

An important conclusion in this study is that screw reinforcement leads to a more ductile, safer failure. It may not be worth using the screws with partial thread for increased strength but it is certainly worth using them to restore the ductility after the development cracks and ensure a less brittle failure.

In addition, the proposed calculation method establishes a path to find the moment-resisting capacity of dowel-type connections reinforced by self-tapping screws. The experiment is based on a small sample size, and more repetitions should be performed to reduce the variability in the results that is induced by the inherent material characteristic of wood. Furthermore, the applicability of the proposed method to other configurations of reinforced connections can be achieved with available embedment strength of timber that is reinforced by screw with similar thread configuration and screw to dowel distance.

Acknowledgement

This work was supported by the National Natural Science Foundation of China [NSFC: 51608144]; the Time For Timber Ltd consulting company; and the Simpson Strong Tie Company Inc.

References

[1] A. D'Ambrisi, F. Focacci, R. Luciano, Experimental investigation on flexural behavior of timber beams repaired with CFRP plates, Composite Structures 108 (2014) 720-728.

[2] G. Metelli, M. Preti, E. Giuriani, On the delamination phenomenon in the repair of timber beams with steel plates, Construction and Building Materials 102 (2016) 1018-1028.

[3] B. Pizzo, M. Gavioli, M.P. Lauriola, Evaluation of a design approach to the on-site structural repair of decayed old timber end beams, Engineering Structures 48 (2013) 611-622.

[4] I. Bejtka, H. Blaß, Self-tapping screws as reinforcements in connections with dowel-type fasteners, International Council for Research and Innovation in Building and Construction-Working Commission W18-Timber Structure (CIB-W18), Universität Karlsruhe, Karlsruhe, Germany, 2005.

[5] H.J. Blaß, P. Schädle, Ductility aspects of reinforced and non-reinforced timber joints, Engineering Structures 33(11) (2011) 3018-3026.

[6] H.J. Blaß, M. Schmid, Self-tapping screws as reinforcement perpendicular to the grain in timber connections, in: S. Aicher, H.W. Reinhardt (Eds.) RILEM Symposium: Joints in Timber Structures, RILEM, Stuttgart, Germany, 2001, pp. 163-172.

[7] M. Closen, F. Lam, Performance of moment resisting self-tapping screw assembly under reverse cyclic load, World Conference on Timber Engineering, Auckland, New Zealand, 2012, pp. 433-440.

[8] M. Gehloff, M. Closen, F. Lam, Reduced edge distances in bolted timber moment connections with perpendicular to grain reinforcements, World Conference on Timber Engineering, 2010.

[9] F. Lam, M. Gehloff, M. Closen, Moment-resisting bolted timber connections, Proceedings of the Institution of Civil Engineers-Structures and Buildings 163(4) (2010) 267-274.

[10] F. Lam, M. Schulte-Wrede, C. Yao, J. Gu, Moment resistance of bolted timber connections with perpendicular to grain reinforcements, 10th World Conference on Timber Engineering Miyazaki, Japan, 2008.

[11] C. Zhang, W. Chang, R. Harris, Investigation of thread configuration for self-tapping screws as reinforcement for embedment strength, International Network on Timber Engineering Research, University of Zagreb, Šibenik, Croatia, 2015, pp. 449-451.

[12] C. Zhang, W. Chang, R. Harris, Investigation of thread configuration of self-tapping screws as reinforcement for dowel-type connection, World Conference on Timber Engineering 2016, University of Vienna, Vienna, Austria, 2016, pp. 1440-1448.

[13] S. Delahunty, Y.H. Chui, M. McCormick, Use of double-threaded self-tapping screws for in-situ repair of cracked timber connecitons, World Conference on Timber Engineering, Quebec City, Canada, 2014.

[14] K. Sawata, M. Yasumura, Determination of embedding strength of wood for dowel-type fasteners, Journal of Wood Science 48(2) (2002) 138-146.

[15] C. Sandhaas, G. Ravenshorst, H. Blass, J. Van de Kuilen, Embedment tests parallel-to-grain and ductility aspects using various wood species, European Journal of Wood and Wood Products 71(5) (2013) 599-608.

[16] B.-H. Xu, A. Bouchaïr, M. Taazount, P. Racher, Numerical simulation of embedding strength of glued laminated timber for dowel-type fasteners, Journal of Wood Science 59(1) (2013) 17-23.

[17] S. Franke, N. Magnière, The embedment failure of European beech compared to spruce wood and standards, Materials and Joints in Timber Structures, Springer2014, pp. 221-229.

[18] T. Reynolds, B. Sharma, K. Harries, M. Ramage, Dowelled structural connections in laminated bamboo and timber, J Composites Part B: Engineering 90 (2016) 232-240.

[19] C. Echavarría, Bolted timber joints with self-tapping screws, Revista EIA (8) (2007) 37-47.

[20] W. Lederer, T.K. Bader, G. Unger, J. Eberhardsteiner, Influence of different types of reinforcements on the embedment behavior of steel dowels in wood, European Journal of Wood and Wood Products 74(6) (2016) 793-807.

[21] OIB, European Technical Approval ETA-13/0796 of 15.12.2017, Österreichische Institut für Bautechnik (OIB), 2017.

[22] BSI (2004) BS EN 1995-1-1:2004+A2:2014. Eurocode 5: Design of timber structures. General. Common rules and rules for buildings. BSI, London, United Kingdom.

[23] H.J. Blaß, Timber engineering. Step 1: basis of design, material properties, structural components and joints, 1995.

[24] J. Porteous, A. Kermani, Structural timber design to Eurocode 5, John Wiley & Sons2013.

[25] BSI (2007) BS EN 383:2007. Timber structures. Test methods. Determination of embedment strength and foundation values for dowel type fasteners. BSI, London, United Kingdom.

[26] BSI (2016) BS EN 14358:2016. Timber structures. Calculation and verification of characteristic values. BSI, London, United Kingdom.